

Crossover in charge transport from one-dimensional copper-oxygen chains to two-dimensional ladders in $(\text{La}, \text{Y})_y(\text{Sr}, \text{Ca})_{14-y}\text{Cu}_{24}\text{O}_{41}$

T. Ivek,^{*} T. Vuletić, B. Korin-Hamzić, O. Milat, and S. Tomić
Institut za fiziku, P.O. Box 304, HR-10001 Zagreb, Croatia

B. Gorshunov[†] and M. Dressel
1. Physikalisches Institut, Universität Stuttgart, D-70550 Stuttgart, Germany

J. Akimitsu and Y. Sugiyama
Department of Physics, Aoyama-Gakuin University, Setagaya-ku, Tokyo 157-8572, Japan

C. Hess and B. Büchner
Leibniz-Institut für Festkörper- und Werkstoffforschung, D-01171 Dresden, Germany
 (Received 2 June 2008; revised manuscript received 8 September 2008; published 7 November 2008)

The charge transport in the copper-oxygen chain/ladder layers of $(\text{La}, \text{Y})_y(\text{Sr}, \text{Ca})_{14-y}\text{Cu}_{24}\text{O}_{41}$ is investigated along two crystallographic directions in the temperature range from 50 to 700 K and for doping levels from $y \approx 6$ (number of holes $n_h < 1$) to $y=0$ (number of holes $n_h=6$). A crossover from a one-dimensional hopping transport along the chains for $y \geq 3$ to a quasi-two-dimensional charge conduction in the ladder planes for $y \leq 2$ is observed. This is attributed to a partial hole transfer from chains to ladders when the hole doping exceeds $n_h \approx 4$ and approaches fully doped value $n_h=6$. For $y \leq 2$ a weak dielectric relaxation at radio frequencies and a microwave mode are detected, which might be recognized as signatures of a charge-density wave phase developed at short length scales in the ladder planes.

DOI: [10.1103/PhysRevB.78.205105](https://doi.org/10.1103/PhysRevB.78.205105)

PACS number(s): 74.72.Jt, 71.27.+a, 72.20.Ee, 71.45.Lr

I. INTRODUCTION

The spin-ladder and spin-chain systems $(\text{La}, \text{Y})_y(\text{Sr}, \text{Ca})_{14-y}\text{Cu}_{24}\text{O}_{41}$ belong to a vast class of strongly correlated materials, transition-metal oxides, which exhibit some of the most intriguing phenomena in condensed-matter physics.¹ The huge literature on the topics of spin chains and spin ladders accumulated in the last decade (for a review see Ref. 2) has been triggered by the discovery of superconductivity under pressure in the compound $\text{Sr}_{14-x}\text{Ca}_x\text{Cu}_{24}\text{O}_{41}$, $x=13.6$, mostly since this system is the first superconducting copper oxide material with a non-square-lattice.³ The parent material, $\text{Sr}_{14}\text{Cu}_{24}\text{O}_{41}$, of this cuprate superconductor is a charge-density wave (CDW) insulator with a spin gap.⁴⁻⁷ Substituting isovalent Ca for Sr suppresses the CDW insulating phase as shown by dc and ac transport measurements,⁸ while the spin gap remains constant.^{2,7} Nevertheless, recent resonant soft x-ray scattering results⁹ indicate that the CDW might stabilize even for the highest Ca substitution but with a different periodicity indicating strong commensurability effects. When for the compounds with high Ca content external pressure is applied, the spin gap decreases in size but remains finite even when SC sets in.¹⁰ Applying pressure also increases interladder coupling leading to metallic transport along both the legs and rungs of the ladders,¹¹ as well as raises the number of mobile quasiparticles at low temperature.^{12,13} These particles have a finite density of states at the Fermi level and might contribute to the superconducting instability. All these results together with an indication for the existence of a Hebel-Slichter coherence peak in the SC state as well as the significant level of disorder in the doped ladders of $\text{Sr}_{14-x}\text{Ca}_x\text{Cu}_{24}\text{O}_{41}$ indicate that the su-

perconducting pairing mechanism and symmetry are probably different compared to theoretical predictions for pure single ladders.

By now it is well understood that the amount of doped holes and their distribution between chains and ladders determine electronic phases and the spin and charge dynamics. In the fully doped material $\text{Sr}_{14}\text{Cu}_{24}\text{O}_{41}$ the total number of holes (n_h) is 6 per formula unit. The hole distribution between chains and ladders is probed most directly by the polarization-dependent near-edge x-ray absorption fine structure (NEXAFS): at room temperature (RT) according to Nücker *et al.*¹⁴ there is close to 1 hole per formula unit transferred in the ladders (equivalent to $\delta=0.07$ holes per ladder copper site) and about five remain in the chains. Very recently, a quite different distribution of close to 3 holes per formula unit on both ladders and chains was suggested by Rusydi *et al.*¹⁵ The two-dimensional (2D) ladders present a dominant charge transport channel: RT conductivity along the c axis is $\sigma_{dc}(c) \approx 500 \Omega^{-1} \text{cm}^{-1}$ and along the a axis $\sigma_{dc}(a) \approx 20 \Omega^{-1} \text{cm}^{-1}$. Although $\sigma_{dc}(c)$ is rather high, it shows an insulating behavior, i.e., it decreases with lowering temperature down to the charge-density wave phase transition; a similar behavior is found in $\sigma_{dc}(a)$ as well.¹⁶ At the same time, the remaining holes in the chains negligibly contribute to the charge transport: spin dimers are formed between those Cu^{2+} spins that are separated by a localized Zhang-Rice singlet (Cu^{3+}), that is, a site occupied by a localized hole. In this way the antiferromagnetic (AF) dimer pattern is created in chains together with the charge order (CO), both inducing gaps in the spin and charge sector, respectively.¹⁷⁻²¹ On the other hand, in the underdoped materials $(\text{La}, \text{Y})_y(\text{Sr}, \text{Ca})_{14-y}\text{Cu}_{24}\text{O}_{41}$ ($n_h=6-y$) the absence of

holes in ladders eliminates the ladder CDW phase and suppresses the charge-ordered gapped state in chains in favor of disorder-driven insulating phase with charge transport by variable range hopping (VRH).^{22,23} The hopping transport originates in the nonperiodic potential in which holes reside and which is induced by strong local distortions of the chains due to the irregular coordination of La^{3+} , Y^{3+} , Sr^{2+} , and Ca^{2+} ions. The VRH conductivity can then be explained as a result of the distorted distribution of microscopic conductivities, as predicted in Anderson's localization theory. In short, the copper-oxygen chains in the underdoped quasi-one-dimensional (quasi-1D) cuprates can be considered a one-dimensional system in which disorder, associated with random distribution of holes, causes the Anderson localization.

In our previous work^{2,22,23} we have suggested that these results reveal an intriguing possibility for the existence of a phase transition close to $n_h=6$ in the phase diagram of $(\text{La}, \text{Y})_y(\text{Sr}, \text{Ca})_{14-y}\text{Cu}_{24}\text{O}_{41}$ compounds and that further experiments on materials with very low La/Y content, which corresponds to $n_h \leq 6$, should elucidate our proposal. In this paper we attempt to answer this intriguing question on how and why and at which doping level the one-dimensional hopping transport along the chains crosses over into a quasi-two-dimensional charge conduction in the ladder planes. In order to clarify this issue, we have undertaken dc and ac conductivity-anisotropy measurements on single crystals of $(\text{La}, \text{Y})_y(\text{Sr}, \text{Ca})_{14-y}\text{Cu}_{24}\text{O}_{41}$ with different La/Y content (a particular emphasis was put on La/Y contents approaching $y=0$) in a wide frequency and temperature range. We show that for the systems with $y \leq 2$ ($n_h \geq 4$) variable-range hopping fails as a relevant picture for the observed conductivity and that the charge sector bears features encountered in the fully doped systems: conductivity anisotropy is of similar order of magnitude and the logarithmic derivative of resistivity presents (wide) maxima. These results suggest that in the underdoped systems with doping levels $n_h \geq 4$ ladders start contributing to charge transport properties and prevail over chains as an electrical transport channel. Concomitantly, frequency-dependent conductivity seems to indicate that charge ordering at short scales starts to develop in the ladders.

II. SAMPLE CHARACTERIZATION AND EXPERIMENTAL METHODS

High-quality single crystals of materials with low Y content were synthesized: $y=0$ ($\text{Sr}_{14}\text{Cu}_{24}\text{O}_{41}$), $y=0.55$ ($\text{Y}_{0.55}\text{Sr}_{13.45}\text{Cu}_{24}\text{O}_{41}$), and $y=1.6$ ($\text{Y}_{1.6}\text{Sr}_{12.4}\text{Cu}_{24}\text{O}_{41}$). Samples were characterized by powder x-ray diffraction, and Y content was determined by an electron probe microanalyzer. In this study needlelike samples of about 0.4 mm^3 in size were used, cut out of bulk single crystals of these materials, together with previously synthesized $y=3$ ($\text{La}_3\text{Sr}_3\text{Ca}_8\text{Cu}_{24}\text{O}_{41}$) and $y=5.2$ ($\text{La}_{5.2}\text{Ca}_{8.8}\text{Cu}_{24}\text{O}_{41}$). Crystallographic orientation of crystals used in the resistivity anisotropy measurements was determined by taking x-ray backreflection Laue patterns and their subsequent simulation using ORIENTEXPRESS 3.3 software.²⁴ Simulated meshes of two overlapping sublattice unit cells ($a=11.47 \text{ nm}$,

$b=13.37 \text{ nm}$, $c_L=3.93 \pm 0.03 \text{ nm}$, and $Fmmm$ for ladders; and $a=11.47 \text{ nm}$, $b=13.37 \text{ nm}$, $c_C=2.73 \pm 0.03 \text{ nm}$, and $Amma$ for chains) fitted well with the recorded patterns in case of proper crystallographic alignment. The same crystallographic orientations were found in all single crystals: the crystallographic ac plane was found to be parallel to the largest faces of the needlelike prismatic shape crystals: either c axis or a axis was properly oriented lengthwise along the needle axis. Dc resistivity was measured between 50 and 700 K.

A HEWLETT PACKARD 4284A and an AGILENT 4294A impedance analyzers were used to measure complex conductivities of $y=0$, 0.55, and 1.6 at frequencies between 20 Hz and 10 MHz.²⁵ The data at the lowest frequency matched our four-probe dc measurements. The complex dielectric function at frequencies $5\text{--}25 \text{ cm}^{-1}$ was obtained by complex transmission measurements using a coherent-source terahertz spectrometer.²⁶ For latter measurements crystals with plane-parallel faces were prepared by polishing, with thickness of about 0.5 mm and of transverse dimensions about $7 \times 7 \text{ mm}^2$. All measurements were done along the two crystallographic axes defining chain and ladder layers: c axis (along the ladders legs and chains) and the a axis (along the ladders rungs).

III. RESULTS AND ANALYSIS

A. dc transport

Figure 1 shows the behavior of dc resistivity and its logarithmic derivative for different La/Y content ranging from $y=5.2$ to 0 along the c axis [panels (a) and (b)] and the a axis [panels (c) and (d)] in the wide temperature range from 50 K (the lowest temperature obtained in our experiment) up to 700 K. While for two compounds with high $y=5.2$ and 3 the dc resistivity curves along the c axis and the a axis markedly differ below about 300 K, the one along the c axis presenting a much smaller increase with lowering temperature, one finds an almost identical behavior of dc resistivity along the both axes for $y=1.6$, 0.55, and 0. An immediate conclusion that can be drawn from observed behaviors is that the conductivity anisotropy becomes significantly enhanced for high La/Y content $y \geq 3$ (i.e., low hole count $n_h \leq 3$), whereas it remains small and temperature independent for low y (high n_h), as depicted in Fig. 2. The qualitative difference between the two kinds of behavior is emphasized in Fig. 2, which shows conductivity anisotropies normalized to the corresponding RT values. The conductivity anisotropy at RT is in the range of 1–30 and basically does not correlate with La/Y content.

The next significant difference between low and high La/Y contents is found in the temperature dependence of the dc conductivity curves. As already reported for $y=5.2$ and 3, the dc conductivity along the c axis $\sigma_{dc}(c)$ follows a variable-range hopping behavior with the dimension of the system $d=1$ and crosses over around T_{co} to nearest-neighbor hopping at high temperatures.^{2,22,23} The observation of $d=1$ type of VRH conduction is in accord with a rather small interchain coupling in $(\text{La}, \text{Y})_y(\text{Sr}, \text{Ca})_{14-y}\text{Cu}_{24}\text{O}_{41}$. Conversely, VRH fits

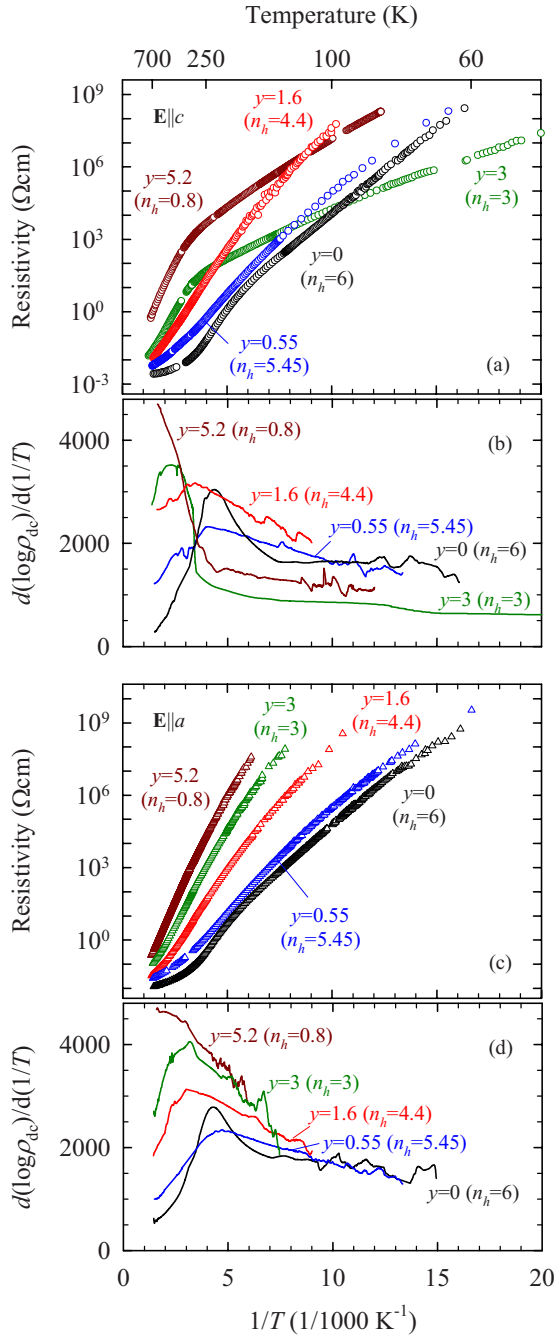


FIG. 1. (Color online) dc resistivity and logarithmic derivatives of $(\text{La}, \text{Y})_y(\text{Sr}, \text{Ca})_{14-y}\text{Cu}_{24}\text{O}_{41}$ for various La/Y content y along the c [panels (a) and (b)] and the a [panels (c) and (d)] crystallographic directions.

$$\sigma_{\text{dc}}(T) = \sigma_0 \exp\left[-\left(\frac{T_0}{T}\right)^{1/(1+d)}\right] \quad (1)$$

to the $\sigma_{\text{dc}}(c)$ curves for $y=1.6$ and 0.55 fail to give a meaningful description: the respective values of the VRH activation energy $T_0^{\text{expt}}=13\,400$ and $9\,000$ meV, obtained from the fit of our data by expression (1) are much larger than those for $y=5.2$ and 3 . This result is at variance with the behavior expected in the VRH mechanism: the more conductive the

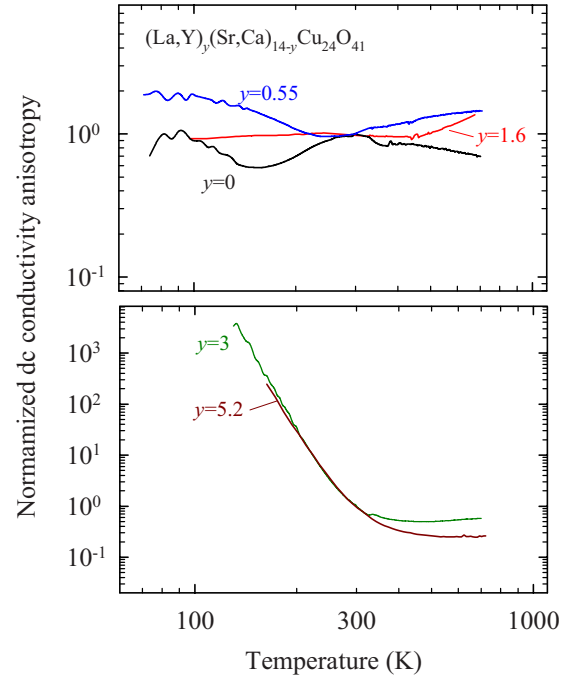


FIG. 2. (Color online) Temperature dependence of the conductivity anisotropy of $(\text{La}, \text{Y})_y(\text{Sr}, \text{Ca})_{14-y}\text{Cu}_{24}\text{O}_{41}$ for various La/Y content y normalized to the corresponding room temperature value.

sample, the lower T_0 is expected. Indeed, these T_0^{expt} values are markedly different from the ones expected theoretically: $T_0^{\text{th}}=2\Delta c_c \alpha \approx 1900$ and 700 meV, see Table I. Here the energy of sites available for hops near the Fermi energy has a uniform distribution in the range $-\Delta$ to Δ , c_c is the distance between the nearest Cu chain sites and $\alpha^{-1}=2c_c T_{\text{co}}/\Delta$ is the localization length. In particular, the experimental values T_0^{expt} are so high that the usual interpretation of the hopping parameters also leads to values too low for the density of states for $y=1.6$ and 0.55 when compared with $y=5.2$ and 3 . It can be noted that the one-dimensional VRH conducting channel along the c axis, which is present in $y \geq 3$, is more efficient when compared with the transport in $y < 3$.

Comparing compounds with high and low y the behavior of dc resistivity along the a axis, $\rho_{\text{dc}}(a)$, differs in a manner that is qualitatively alike $\rho_{\text{dc}}(c)$. The slope of $\log \rho_{\text{dc}}$ vs T^{-1} curves for $y=5.2$ and 3 shows that the activation energy is much larger at high temperatures and becomes smaller with decreasing T , whereas for $y=0.55$ and 0 we find an opposite behavior: a smaller activation energy at high temperatures and a larger one at low temperatures. It appears that the $y=1.6$ compound is situated somewhere at the border between these two distinct behaviors. We recall that for $y=0$ a smaller activation energy at high temperatures and a larger at low temperatures are features associated with an insulator-to-insulator phase transition into the CDW phase in the ladders.¹⁶

Another difference between compounds with low and high y contents becomes obvious when looking at the logarithmic derivative curves [Fig. 1, panels (b) and (d)]. For $y=0.55$ (but not $y=3$ and 5.2), both $\mathbf{E}\parallel a$ and $\mathbf{E}\parallel c$ orientations show a broad and flat maximum in $d(\ln \rho)/d(1/T)$ centered at about 210 K, similar to $y=0$ where this feature, albeit

TABLE I. dc transport parameters of $(\text{La}, \text{Y})_y(\text{Sr}, \text{Ca})_{14-y}\text{Cu}_{24}\text{O}_{41}$ for various La/Y content y along the c axis.

| Compound | y | Δ (meV) | T_{co} (K) | T_0^{expt} (meV) | α^{-1} (Å) | T_0^{th} (meV) |
|--|------|-------------------|------------------------|------------------------------|----------------------|----------------------------|
| $\text{Y}_{0.55}\text{Sr}_{13.45}\text{Cu}_{24}\text{O}_{41}$ | 0.55 | 130 ± 40 | 280 ± 15 | 9000 ± 100 | 0.960 | 750 |
| $\text{Y}_{1.6}\text{Sr}_{12.4}\text{Cu}_{24}\text{O}_{41}$ | 1.6 | 230 ± 10 | 330 ± 30 | 13400 ± 100 | 0.677 | 1900 |
| $\text{La}_3\text{Sr}_3\text{Ca}_8\text{Cu}_{24}\text{O}_{41}$ | 3 | 280 ± 10 | 295 ± 5 | 2500 ± 100 | 0.481 | 3400 |
| $\text{La}_{5.2}\text{Ca}_{8.8}\text{Cu}_{24}\text{O}_{41}$ | 5.2 | 370 ± 50 | 330 ± 5 | 4300 ± 100 | 0.435 | 4600 |

more narrow, is recognized as a signature of the CDW phase transition in the ladders. This feature remains visible for $y = 1.6$; however it is now extremely broad and flat, shifted to 300 K and more pronounced for $\mathbf{E} \parallel a$ than in $\mathbf{E} \parallel c$ orientation.

Finally, an unusual result concerns the magnitude of RT conductivity²⁷ along both axes which increases substantially with total hole count (see Fig. 3). It is evident that the increased number of holes per formula unit cannot account completely for this orders-of-magnitude rise in conductivity. Theoretically, doping could create a finite density of states at the Fermi level by shifting the Fermi level from the gap into the region with high density of states, which then might partially account for the observed conductivity rise. Nevertheless, an overall rise hints to an extraordinary increase in mobility which happens for y smaller than two.

B. ac conductivity and dielectric function

We now turn to other features derived from a comparative analysis of dc and ac conductivity data. The conductivity spectra of $(\text{La}, \text{Y})_y(\text{Sr}, \text{Ca})_{14-y}\text{Cu}_{24}\text{O}_{41}$ for $y = 0.55$ and 1.6 in the frequency range between 5 and 25 cm^{-1} at several representative temperatures are shown in Fig. 4. An almost dispersionless conductivity spectrum at RT revealing the existence of a metallic response of $y = 0$ in the infrared conductivity along both c and a axes (see Fig. 67 in Ref. 2) is also evident for $y = 0.55$ and 1.6.²⁸ This result indicates the

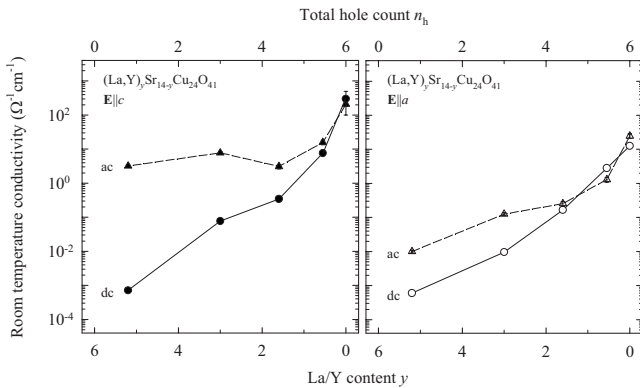


FIG. 3. Room temperature dc (circles) and ac conductivity at 10 cm^{-1} (triangles) (Ref. 27) along the c axis (left panel) and the a axis (right panel) as a function of La/Y content y and total hole count n_h . The full and dashed lines are guides to the eyes for dc and ac data, respectively.

appearance of a certain amount of free charges not detected for $y = 3$ and 5.2 (see inset of Fig. 3 of Ref. 22) and indicates that the observed spectra could be attributed to the charge excitations in the ladders similarly as for $y = 0$.² We will address this behavior once more at the end of this section. On lowering the temperature below 200 K, a suppression of the Drude weight is clearly visible in the conductivity spectra along the c and a axes indicating that an insulating behavior develops.

We note that in all studied cases (here we point out in particular $y = 0.55$ and 1.6) the conductivity behavior in the

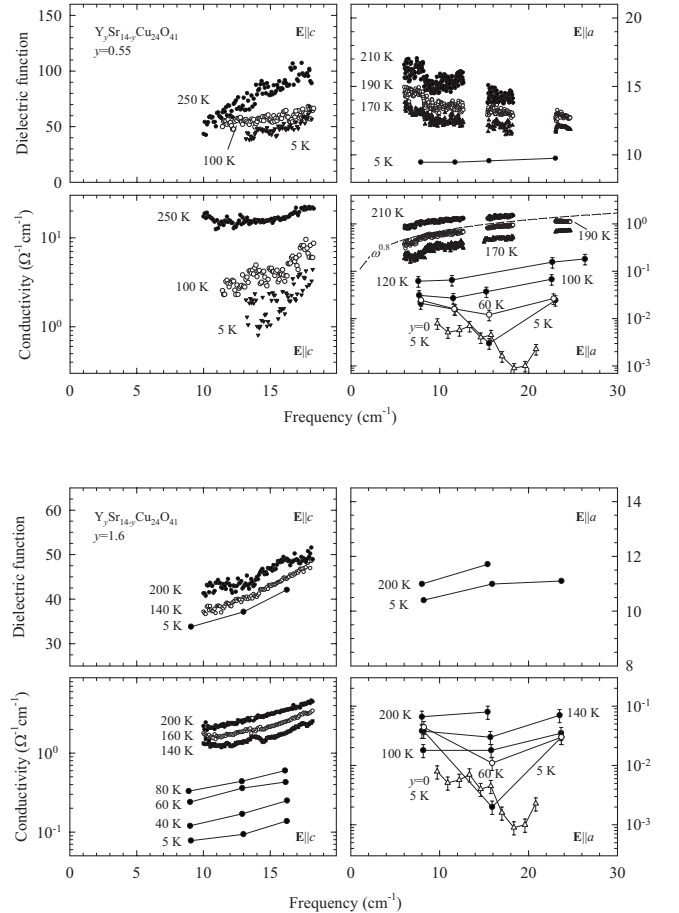


FIG. 4. Dielectric function and infrared conductivity in terahertz region of $\text{Y}_y\text{Sr}_{14-y}\text{Cu}_{24}\text{O}_{41}$ for various Y content $y = 0.55$ (upper panel) and 1.6 (lower panel) along the c and a axes at several temperatures as indicated. Conductivity data for $y = 0$ along the a axis at 5 K (denoted as open triangles) are shown for comparison.

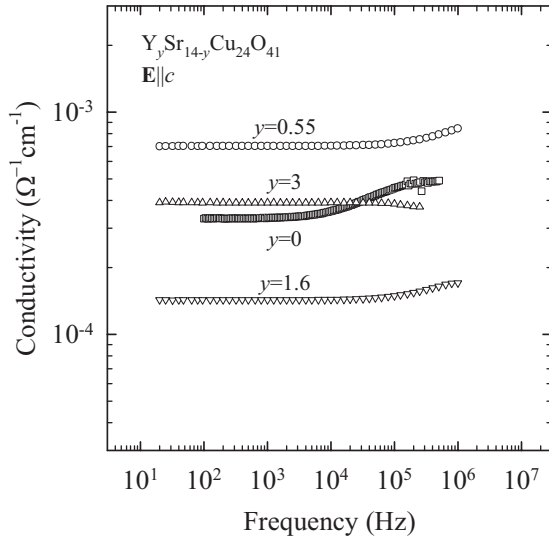


FIG. 5. Conductivity spectra of $y=0, 0.55, 1.6,$ and $3, \mathbf{E}\parallel c$ in the radio-frequency range at representative temperatures (95, 125, 165, and 132.5 K, respectively) with comparable dc conductivities.

dc limit (see Fig. 1) is followed by a conductivity rise leading to a relatively high ac conductivity in the infrared, as compared to the dc conductivity. A mechanism standardly responsible for such a conductivity rise is electronic hopping conduction characterized by a power-law dispersion $\sigma_{ac}(T) \propto A(T)\omega^s$. Indeed, hopping conduction with $s \approx 1$ has already been established in the ladders of $y=0$ compound for $\mathbf{E}\parallel c$ and $\mathbf{E}\parallel a$, as well as in the chains of $y=3$ and 5.2 for $\mathbf{E}\parallel c$.^{2,22,23} In this study, the power-law behavior is found only for $y=0.55$ ($\mathbf{E}\parallel a$) between 200 and 100 K, freezing out at lower temperatures. There are two reasons which prevented detection of hopping conduction for other cases. The first is related to the phonon tail masking the hopping dispersion for $\mathbf{E}\parallel c$ orientation.²⁹ Indeed, for the c -axis response of $y=0.55$ and 1.6 , at the lowest temperature ($T=5$ K) we see a typical phonon tail in the terahertz range. It seems that for these two compositions the lowest-frequency phonon sits at about 25 cm^{-1} , i.e., at the same frequency where the lowest-frequency phonon for the $y=3$ (see Fig. 3 of Ref. 22) and for $\text{Sr}_{11}\text{Ca}_3\text{Cu}_{24}\text{O}_{41}$ compound was found. The second reason preventing electronic hopping detection for $\mathbf{E}\parallel a$ below about 100 K is due to a clear conductivity increase below 20 cm^{-1} . We propose that this increase might be an indication of a pinned CDW mode located in the microwave range. It is noteworthy that this feature is also visible for $y=0$ compound (see Fig. 4 for $\mathbf{E}\parallel a$). Having only the higher-frequency slope of the mode we cannot make a quantitative fit and determine parameters such as eigenfrequency, dielectric strength, and damping. Nevertheless, estimates based on our dielectric function and conductivity data indicate that these parameters would be much different from those of the pinned CDW mode at 1.8 cm^{-1} as inferred by Kitano *et al.*³⁰ for fully doped compound $\text{Sr}_{14}\text{Cu}_{24}\text{O}_{41}$ based on some distinct microwave points and as discussed at length in Ref. 2. On the other hand, for $\mathbf{E}\parallel c$ we do not detect any signature of this pinned mode in the terahertz range, which might be either due to its location at lower frequencies or the mode

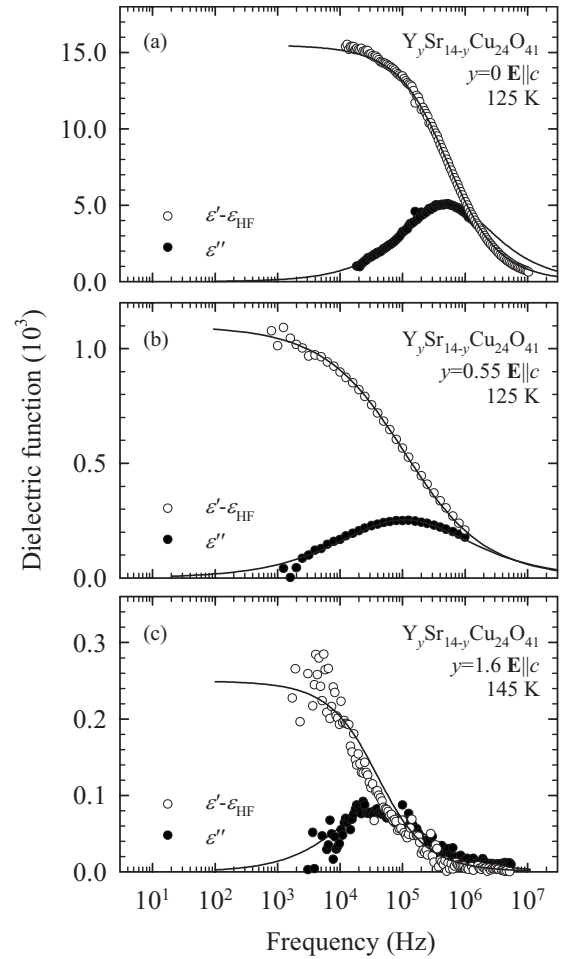


FIG. 6. Real (ϵ') and imaginary (ϵ'') parts of the dielectric function of $\text{Y}_y\text{Sr}_{14-y}\text{Cu}_{24}\text{O}_{41}$ for $y=0$ [panel (a)], $y=0.55$ [panel (b)], and $y=1.6$ [panel (c)] at representative temperatures of 125 K ($y=0$ and 0.55) and 145 K ($y=1.6$) as a function of frequency, with the ac electric field applied along the c axis. The full lines are fits to data using the generalized Debye expression $\epsilon(\omega) - \epsilon_{\text{HF}} = \Delta\epsilon / [1 + (i\omega\tau_0)^{1-\alpha}]$.

being masked by a contribution of free carriers or a nearby phonon. It is noteworthy that this mode, which we tentatively attribute to the pinned CDW mode, is absent in the terahertz spectra of $y=3$ and 5.2 compounds. This behavior indicates that an alternative assignment of the CDW pinned mode emerging from our data, although at delicate grounds due to a very narrow frequency range, might be of relevance which should not be neglected. The issue of pinned CDW mode and its evolution in $\text{Y}_y\text{Sr}_{14-y}\text{Cu}_{24}\text{O}_{41}$ obviously deserves more attention in the future. As far as dielectric constant ϵ' of $y=0.55$ and 1.6 is concerned, we note that it coincides well with the dielectric constant of the fully doped compound $\text{Sr}_{11}\text{Ca}_3\text{Cu}_{24}\text{O}_{41}$ (see Fig. 66 of Ref. 2), meaning that the infrared phonon spectra of all these three materials could be very similar.

We turn now to the radio-frequency results. While for $y=0$ compound the CDW develops in the ladders yielding a pronounced steplike conductivity increase in the radio-frequency range, the frequency dependence is much weaker for $y=0.55$ and 1.6 and even comparable to $y=3$ compound

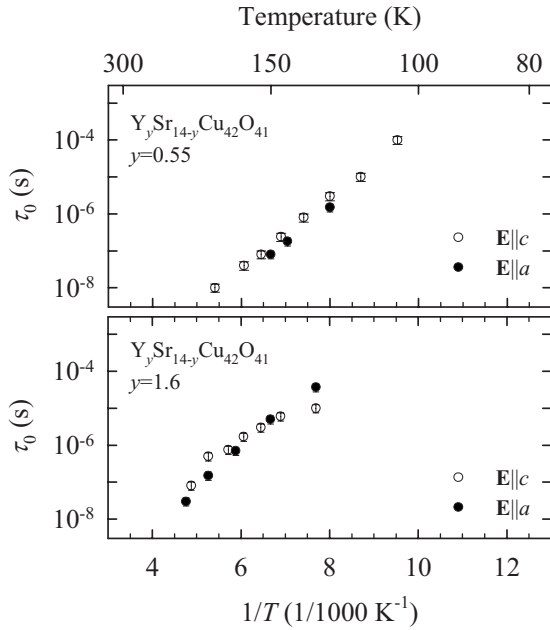


FIG. 7. Temperature dependence of mean relaxation times τ_0 for $y=0.55$ and 1.6 . Open and full circles are for $\mathbf{E}\parallel c$ and $\mathbf{E}\parallel a$, respectively.

(see Fig. 5). We recall that for $y=3$ as well as for $y=5.2$ the frequency independent behavior is found in the radio-frequency range for all temperatures.^{2,22,23} However, unlike for $y=3$ and 5.2 , when the complex dielectric function for $y=0.55$ and 1.6 is calculated from complex conductivity, a weak dielectric relaxation mode emerges (see Fig. 6): a characteristic steplike drop in the real part of dielectric function and a wide maximum in the imaginary part, resembling that of the fully doped $\text{Sr}_{14}\text{Cu}_{24}\text{O}_{41}$ parent system ($y=0$) where CDW is fully developed. A similar behavior is observed for both polarizations $\mathbf{E}\parallel c$ and $\mathbf{E}\parallel a$, as in the case of $y=0$. Also, the mean relaxation time τ_0 has comparable values and temperature dependence when measured along both the c and a axes (Fig. 7).^{2,16} However, contrary to the $y=0$ case, the temperature range in which we were able to track the mode for $y=0.55$ and 1.6 was rather narrow (see Fig. 7). Still, a systematic trend in the behavior upon doping is clearly visible. In this range the dielectric strength is small (10^3 and 10^2 for $y=0.55$ and 1.6 , respectively) when compared to the value for $y=0$ (10^4 at same temperatures). Another worrisome issue is that because of the small low-frequency capacitance we were not able to follow its disappearance. Nevertheless, we are tempted to qualitatively associate this weak mode with a ladder CDW order which persists only at short length scales for $y=0.55$ and 1.6 , whereas it fully disappears for $y=3$ and 5.2 .

Finally, coming back to the crossover from metallic to insulating behavior upon doping (i.e., increasing y), we compare the RT ac conductivity at 10 cm^{-1} with dc conductivity and find the following interesting feature (see Fig. 3). RT conductivity data clearly show how the metalliclike character of charge transport in $y=0$ (σ_{ac} is close to σ_{dc}) gradually deteriorates with y (σ_{ac} values differ from σ_{dc}) and becomes typical for dielectrics for $y=3$ and 5.2 . It is hard to quantify

where this change starts since for $y=0.55$ and 1.6 the highest temperatures at which σ_{ac} was measured were 210 and 250 K, respectively,²⁷ so that actual RT σ_{ac} are higher than those shown in Fig. 3. Taking this into account, the dc and ac conductivity contributions differ substantially along both orientations for $y \gtrsim 2$, i.e., when the total hole count is smaller than four. At temperatures lower than about 200 K, reliable estimates of infrared conductivity are prevented due to either a phonon or a pinned CDW-like mode influence so that we can only make crude estimates. However, we can say that $\sigma_{ac}(10\text{ cm}^{-1})/\sigma_{dc}$ ratio for all La/Y contents increases with lowering temperature indicating the evolution of the insulating behavior.

IV. DISCUSSION

From the above analysis we conclude that the one-dimensional hopping transport along the chains for $2 < y \leq 6$ (hole doping from zero to three injects holes uniquely into chains) crosses over into a quasi-two-dimensional charge conduction in ladders for smaller y . Supports for this conjecture are a weak and temperature-independent conductivity anisotropy (see Fig. 2) for $0 \leq y \leq 1.6$; a maximum in $d(\ln \rho)/d(1/T)$ centered around 210 K (see Fig. 1) which becomes broader and flatter going from $y=0$ to 1.6 ; a smaller activation energy at high temperatures and larger at low temperatures: this difference disappears for $y=1.6$.

These results might be attributed to the CDW whose long-range order (with coherence length of about 260 \AA) as developed in $y=0$ compound⁶ is destroyed, but domains developed at short-range scale still persist until $y \approx 1.6$. Indeed, a weak dielectric relaxation mode is detected in the radio-frequency range; it resembles a CDW loss peak. The increase in conductivity below 20 cm^{-1} and the considerably larger value compared to the dc conductivity infer some excitation which suggests an additional mode somewhere in the microwave range. One might be tempted to ascribe it to the pinned CDW mode although the parameters seem to be different from those of the peak that was proposed to be the pinned mode in $y=0$ compound.

Further, we remind that neutron-scattering and static susceptibility measurements show that with y increasing from zero to one ($0 < y \leq 1$) AF dimer long-range order in chains (AF dimers separated by a site occupied by a localized hole) is also gradually destroyed.^{31–33} In addition, NMR measurements of spin-lattice relaxation rate revealed that the spin gap associated with AF dimer order in chains persists until $y=2$.⁷ The latter result signals that antiferromagnetic and charge correlations for $y=2$ (total hole count $n_h=4$) are already strong enough that domains of AF dimers and related CO form dynamically and so exist at short time scales. Concomitantly, chains cease to be a favorable charge transport channel and the beginning of hole transfer to ladders is induced. A partial hole transfer from chains into ladders starts once the total hole count becomes close to four and larger. Although probably only a tiny amount of holes is transferred to ladders for $y=1.6$, it appears that the observed conduction with a weak and temperature-independent anisotropy happens predominantly in ladders. For $y=0.55$ it is evident that

the charge transport along the chains is almost completely frozen due to rather well developed AF dimers and CO and taken over by two-dimensional ladders in which transferred amount of holes bears a much larger mobility, yielding an important conductivity rise toward $y=0$.

Our results therefore suggest that ladders at La/Y content $y \lesssim 2$ prevail over chains as the conduction channel. A question arises why do holes, which are doped only into the chains as La/Y content is varied from $y=6$ to $y \approx 2$, start to be distributed between chains and ladders once their total count is larger than 4. In other words, it appears that doping more than four holes in the chains is energetically favorable only if at least a tiny amount of holes is concomitantly doped in the ladders. A subtle interaction between chains and ladders, and stability of respective electronic phases in the charge and spin sectors are already evidenced for fully doped compounds: the chain CO and AF dimer pattern on one side and ladder CDW on the other are both being suppressed at a similar rate.^{2,34} Our results in the underdoped series follow on this idea and additionally reveal that the formation of these two distinct electronic phases is also mutually interdependent, in the sense that one cannot develop without the other.

As a final remark we note that the proposed scenario fits perfectly well to the hole distribution proposed by Nücker *et al.*¹⁴ for $y=0$ compound, $\text{Sr}_{14}\text{Cu}_{24}\text{O}_{41}$: close to 5 holes per formula unit in the chains and close to 1 hole per formula unit in the ladders. However, this hole distribution cannot account for the observed periodicity of CDW in ladders.⁶ Conversely, a hole distribution of close to 3 holes per formula unit in both ladders and chains, recently proposed by Rusydi *et al.*,¹⁵ demonstrates opposite problems in explaining formation of electronic phases in the underdoped series toward fully doped systems when La/Y content decreases from $y=3$ to 0, i.e., when the total hole count increases from 3 to 6. Namely, a gradual doping of holes from zero to three in ladders nicely explains formation of the CDW in ladders and its eventual periodicity found in $y=0$ compound when long-range order is developed. On the other hand, a fixed hole count in chains in the range $0 \leq y < 3$ encounters difficulties to explain short-range AF dimer and CO domains therein, which dynamically appear at $y \approx 2$ and grow in size as La/Y content decreases to $y=0$. It also stays in contradiction with

the susceptibility results, which show that on decreasing y in the range $0 \leq y \leq 3$ the number of spins in chains decreases, meaning a gradual increase in hole count in chains.^{32,33} Obviously, more experimental efforts are needed to clarify and reconcile these contradictory findings in order to construct a self-consistent picture of physics of chains and ladders in $(\text{La}, \text{Y})_y(\text{Sr}, \text{Ca})_{14-y}\text{Cu}_{24}\text{O}_{41}$.

V. CONCLUSION

In conclusion, we demonstrated the crossover from a one-dimensional hopping charge transport in the chain subsystem for $y \geq 3$ to a quasi-two-dimensional charge conduction in the ladder planes for $y \lesssim 2$. We suggest that while holes are doped only into the chains for low hole counts, they are distributed between chains and ladders once the total hole count n_h exceeds 4. We propose that a clue which determines the hole distribution is associated with a mutually interdependent formation of antiferromagnetic dimer and charge order in chains and charge-density wave in ladders. Our results confirm once more a profound interplay between chain and ladder subunits showing clearly that any decent theoretical model attempting to give a proper and self-consistent description of electronic phases in $(\text{La}, \text{Y})_y(\text{Sr}, \text{Ca})_{14-y}\text{Cu}_{24}\text{O}_{41}$ should take this into account.

ACKNOWLEDGMENTS

We thank G. Untereiner for the samples preparation and M. Herak and M. Miljak for useful discussions. This work was supported by the Croatian Ministry of Science, Education and Sports under Grants No. 035-0000000-2836 and No. 035-0352843-2844, the Deutsche Forschungsgemeinschaft (DFG), and by the Program for Fundamental Research "Problems of Radiophysics" of the Department of Physical Sciences, Russian Academy of Sciences. This work was partly supported by the 21st COE program, "High-Tech Research Center" Project for Private Universities: matching fund subsidy from MEXT (Ministry of Education, Culture, Sports, Science and Technology, 2002–2004), and a Grant-in-Aid for Scientific Research on Priority Area from the Ministry of Education, Culture, Sports, Science and Technology of Japan.

*<http://real-science.ifs.hr/>; tivsek@ifs.hr

[†]Permanent address: A. M. Prokhorov General Physics Institute, Russian Academy of Sciences, 119991 Moscow, Russia.

¹S. Maekawa, T. Tohyama, S. E. Barnes, S. Ishihara, W. Koshibae, and G. Khaliullin, *Physics of Transition Metal Oxides* (Springer, Berlin, 2004).

²T. Vuletić, B. Korin-Hamzić, T. Ivek, S. Tomić, B. Gorshunov, M. Dressel, and J. Akimitsu, *Phys. Rep.* **428**, 169 (2006).

³M. Uehara, T. Nagata, J. Akimitsu, H. Takahashi, N. Môri, and K. Kinoshita, *J. Phys. Soc. Jpn.* **65**, 2764 (1996).

⁴B. Gorshunov, P. Haas, T. Rößm, M. Dressel, T. Vuletić, B.

Korin-Hamzić, S. Tomić, J. Akimitsu, and T. Nagata, *Phys. Rev. B* **66**, 060508(R) (2002).

⁵G. Blumberg, P. Littlewood, A. Gozar, B. S. Dennis, N. Motoyama, H. Eisaki, and S. Uchida, *Science* **297**, 584 (2002).

⁶P. Abbamonte, G. Blumberg, A. Rusydi, A. Gozar, P. G. Evans, T. Siegrist, L. Venema, H. Eisaki, E. D. Isaacs, and G. A. Sawatzky, *Nature (London)* **431**, 1078 (2004).

⁷K. I. Kumagai, S. Tsuji, M. Kato, and Y. Koike, *Phys. Rev. Lett.* **78**, 1992 (1997).

⁸T. Vuletić, B. Korin-Hamzić, S. Tomić, B. Gorshunov, P. Haas, T. Rößm, M. Dressel, J. Akimitsu, T. Sasaki, and T. Nagata,

- Phys. Rev. Lett. **90**, 257002 (2003).
- ⁹A. Ruydy, P. Abbamonte, H. Eisaki, Y. Fujimaki, G. Blumberg, S. Uchida, and G. A. Sawatzky, Phys. Rev. Lett. **97**, 016403 (2006).
- ¹⁰Y. Piskunov, D. Jérôme, P. Auban-Senzier, P. Wzietek, C. Bourbonnais, U. Ammerahl, G. Dhalenne, and A. Revcolevschi, Eur. Phys. J. B **24**, 443 (2001).
- ¹¹T. Nagata, M. Uehara, J. Goto, J. Akimitsu, N. Motoyama, H. Eisaki, S. Uchida, H. Takahashi, T. Nakanishi, and N. Mōri, Phys. Rev. Lett. **81**, 1090 (1998).
- ¹²N. Fujiwara, N. Mōri, Y. Uwatoko, T. Matsumoto, N. Motoyama, and S. Uchida, Phys. Rev. Lett. **90**, 137001 (2003).
- ¹³Y. Piskunov, D. Jérôme, P. Auban-Senzier, P. Wzietek, and Y. Yakubovsky, Phys. Rev. B **69**, 014510 (2004).
- ¹⁴N. Nücker, M. Merz, C. A. Kuntscher, S. Gerhold, S. Schuppler, R. Neudert, M. S. Golden, J. Fink, D. Schild, S. Stadler, V. Chakarian, J. Freeland, Y. U. Idzerda, K. Conder, M. Uehara, T. Nagata, J. Goto, J. Akimitsu, N. Motoyama, H. Eisaki, S. Uchida, U. Ammerahl, and A. Revcolevschi, Phys. Rev. B **62**, 14384 (2000).
- ¹⁵A. Ruydy, M. Berciu, P. Abbamonte, S. Smadici, H. Eisaki, Y. Fujimaki, S. Uchida, M. Rübhausen, and G. A. Sawatzky, Phys. Rev. B **75**, 104510 (2007).
- ¹⁶T. Vuletić, T. Ivek, B. Korin-Hamzić, S. Tomić, B. Gorshunov, P. Haas, M. Dressel, J. Akimitsu, T. Sasaki, and T. Nagata, Phys. Rev. B **71**, 012508 (2005).
- ¹⁷M. Matsuda and K. Katsumata, Phys. Rev. B **53**, 12201 (1996).
- ¹⁸M. Matsuda, K. Katsumata, T. Yokoo, S. M. Shapiro, and G. Shirane, Phys. Rev. B **54**, R15626 (1996).
- ¹⁹M. Takigawa, N. Motoyama, H. Eisaki, and S. Uchida, Phys. Rev. B **57**, 1124 (1998).
- ²⁰L. P. Regnault, J. P. Boucher, H. Moudden, J. E. Lorenzo, A. Hiess, U. Ammerahl, G. Dhalenne, and A. Revcolevschi, Phys. Rev. B **59**, 1055 (1999).
- ²¹The main condition to establish AF dimer+CO is that the number of holes in the chains per formula unit is close to 6. This requirement is satisfied according to Ref. 14, while it cannot be reconciled with the hole distribution suggested in Ref. 15.
- ²²T. Vuletić, B. Korin-Hamzić, S. Tomić, B. Gorshunov, P. Haas, M. Dressel, J. Akimitsu, T. Sasaki, and T. Nagata, Phys. Rev. B **67**, 184521 (2003).
- ²³T. Vuletić, T. Ivek, B. Korin-Hamzić, S. Tomić, B. Gorshunov, M. Dressel, C. Hess, B. Büchner, and J. Akimitsu, J. Phys. IV **131**, 299 (2005).
- ²⁴<http://www.ccp14.ac.uk/tutorial/lmgp/orientexpress.htm>
- ²⁵M. Pinterić, T. Vuletić, S. Tomić, and J. U. von Schütz, Eur. Phys. J. B **22**, 335 (2001).
- ²⁶B. Gorshunov, A. Volkov, I. Spektor, A. Prokhorov, A. Mukhin, M. Dressel, S. Uchida, and A. Loidl, Int. J. Infrared Millim. Waves **26**, 1217 (2005).
- ²⁷The measurement of ac conductivity for $y=0.55$ and 1.6 was done at 250 and 200 K, respectively, due to too high conductivity values causing too low transmittivity of prepared plane-parallel samples.
- ²⁸While Drude response is clearly visible at RT for $y=0.55$ ($\mathbf{E}\parallel c$) and $y=1.6$ ($\mathbf{E}\parallel a$) it is masked by the phonon tail for $y=1.6$ ($\mathbf{E}\parallel c$).
- ²⁹We remind that only at low temperatures one standardly expects that due to frozen charge carriers a low-energy phonon contribution prevails over electronic hopping.
- ³⁰H. Kitano, R. Isobe, T. Hanaguri, A. Maeda, N. Motoyama, M. Takaba, K. Kojima, H. Eisaki, and S. Uchida, Europhys. Lett. **56**, 434 (2001).
- ³¹M. Matsuda, K. Katsumata, T. Osafune, N. Motoyama, H. Eisaki, S. Uchida, T. Yokoo, S. M. Shapiro, G. Shirane, and J. L. Zarestky, Phys. Rev. B **56**, 14499 (1997).
- ³²M. Kato, T. Adachi, and Y. Koike, Physica C **265**, 107 (1996).
- ³³M. Herak and M. Miljak (private communication).
- ³⁴V. Kataev, K. Y. Choi, M. Grüninger, U. Ammerahl, B. Büchner, A. Freimuth, and A. Revcolevschi, Phys. Rev. B **64**, 104422 (2001).